Journal of Energy Storage 89 (2024) 111650

Contents lists available at ScienceDirect

Journal of Energy Storage

journal homepage: www.elsevier.com/locate/est

Research Papers

Exploring the electrochemical and physical stability of lithium-ion cells exposed to liquid nitrogen

R. Leonhardt [a,b], N. Böttcher [a,b], S. Dayani [a], A. Rieck [a], H. Markötter [a], A. Schmidt [a], J. Kowal [b], Tim Tichter [a,*], Jonas Krug von Nidda [a,*]

[a] Bundesanstalt für Materialforschung und -prüfung (BAM), Unter den Eichen 87, 12205, Berlin, Germany
[b] Technische Universität Berlin, Institut für Energie- und Automatisierungstechnik, Einsteinufer 11, 10587, Berlin, Germany

ARTICLE INFO

Keywords:
Lithium-ion batteries
Cryogenic cooling
Liquid nitrogen
Battery swelling
Electrochemical characterization
X-ray computed tomography

ABSTRACT

The transport and storage of lithium-ion (Li-ion) batteries — damaged or in an undefined state — is a major safety concern for regulatory institutions, transportation companies, and manufacturers. Since (electro)chemical reactivity is exponentially temperature-dependent, cooling such batteries is an obvious measure for increasing their safety.

The present study explores the effect of cryogenic freezing on the electrochemical and physical stability of Li-ion cells. For this purpose, three different types of cells were repeatedly exposed to liquid nitrogen (LN_2). Before and after each cooling cycle, electrical and electrochemical measurements were conducted to assess the impact of the individual freezing steps. While the electrochemical behavior of the cells did not change significantly upon exposure to LN_2, it became apparent that a non-negligible number of cells suffered from physical changes (swelling) and functional failures. The latter defect was found to be caused by the current interrupt device of the cylindrical cells. This safety mechanism is triggered by the overpressure of expanding nitrogen which enters the cells at cryogenic temperatures.

This study underlines that the widely accepted reversibility of LN_2-cooling on a material scale does not allow for a direct extrapolation toward the physical integrity of full cells. Since nitrogen enters the cell at cryogenic temperatures and expands upon rethermalization, it can cause an internal overpressure. This can, in turn, lead to mechanical damage to the cell. Consequently, a more appropriate temperature condition — less extreme than direct LN_2 exposure — needs to be found.

1. Introduction

While lithium-ion (Li-ion) batteries facilitate numerous technologies contributing to a decarbonized, more sustainable future, they also pose various safety-related questions. Particularly, batteries that are damaged or in an uncertain condition present a significant challenge as they bear the hazard of thermal runaway (TR) and the release of toxic and explosive gas [1,2]. These potential risks are exacerbated during transportation, where environmental factors such as physical vibrations and temperature fluctuations can trigger undesired reactions [3]. To mitigate these hazards, regulatory agencies, transportation companies, and manufacturers are actively developing methods to enhance the safety of Li-ion batteries and their transportation.

As (electro)chemical reaction kinetics are strongly temperature-dependent in an Arrhenius type, cooling down Li-ion batteries is a promising strategy to improve their safety before and during critical events. In this context, it was demonstrated that the use of liquid nitrogen (LN_2, T = −196 °C) can rapidly freeze Li-ion cells down to cryogenic temperatures and thus eliminate their reactivity. Recent studies conducted by Cao et al. [4], and Wang et al. [5] investigated the effects of spraying LN_2 on Li-ion cells as a measure to mitigate the effects of a TR. Their results underline that cooling with LN_2 can eliminate the risks of TR and TR propagation.

On a material scale, a study carried out by Li et al. [6] investigated the effects of low-temperature exposure (i.e., −80 °C) of $LiNi_{1-x-y}Mn_xCo_yO_2$ positives electrodes on their physical stability. It is shown that deformation of the positive electrode lattice can induce irreversible particle cracking, which can further lead to structural disintegration of the positive electrode. The study concludes that this can result in local impedance growth and capacity degradation due to particle deactivation.

The implications of cryogenic cooling on the properties of full Li-ion cells are also the subject of recent research. Studies from Grandjean

* Corresponding authors.
E-mail addresses: tim.tichter@bam.de (T. Tichter), jonas.krug-von-nidda@bam.de (J. Krug von Nidda).

https://doi.org/10.1016/j.est.2024.111650
Received 29 June 2023; Received in revised form 18 March 2024; Accepted 6 April 2024
Available online 19 April 2024

Table 1
Overview of commercial Li-ion cells investigated in this study.

Attribute	Cell type A	Cell type B	Cell type C
Cell type	Gaoneng 1300 mAh-85C	Samsung SDI INR18650-29E	LiFePO4 18650-1600-3.3V
Format	Pouch	Cylindrical	Cylindrical
Positive electrode material	$LiCoO_2$	$LiNi_{0.5}Mn_{0.3}Co_{0.2}O_2$	$LiFePO_4$
Negative electrode material	Graphite	Graphite	Graphite
Nominal capacity	1.3 Ah	2.6 Ah	1.6 Ah

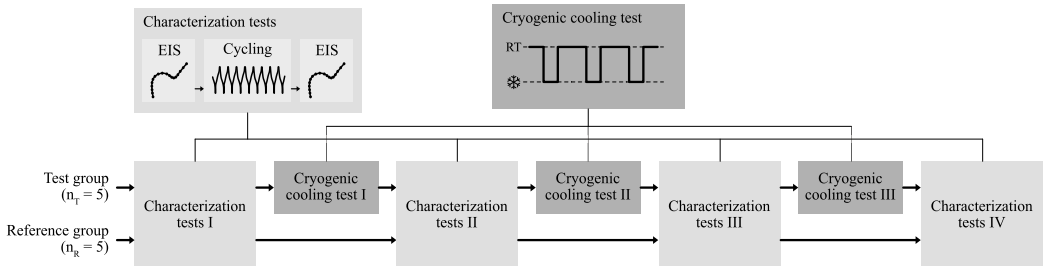

Fig. 1. Main test protocol. The test protocol for the present study consists of three cryogenic cooling tests (each comprising three LN_2 submerging events with resting periods) applied to the test samples ($n_T = 5$). Before and after each cryogenic cooling test, electrochemical characterizations, such as electrochemical impedance spectroscopy (EIS), were conducted. A reference group ($n_R = 5$) was subjected to the same test protocol without the cryogenic cooling tests.

et al. [7,8] and Sunderlin et al. [9] confirm the safety-increasing effects of cryogenic freezing and conclude that any changes in the cells are fully reversible without any remaining damage. A study conducted by Nadini et al. [10], which focuses on the physical durability of 18 650 Li-ion cells, states that freezing them to cryogenic temperatures will not cause significant physical damage. However, the implications of directly exposing Li-ion cells to LN_2 on their physical integrity are not yet sufficiently understood.

The effects of rapid cryogenic freezing on the electrochemical performance and physical integrity of Li-ion cells are thoroughly investigated in the present study. For this purpose, three different commercial cell types ($LiCoO_2$ pouch cell, $LiNi_{0.5}Mn_{0.3}Co_{0.2}O_2$ cylindrical cell, and $LiFePO_4$ cylindrical cell) were directly exposed to LN_2 (i.e., by submerging) and repeatedly characterized electrochemically before and after each cooling period. While the electrochemical behavior — if it can be analyzed — remained almost unchanged, multiple cells showed swelling and functional failures. These were found to be caused by an internal overpressure inside of the cells which builds up during warming the cells up to room temperature (rethermalization), which indicates that nitrogen enters the cell at cryogenic temperatures. This poses major concerns with the LN_2-cooling method as a practically relevant safety measure.

In this manner, the results of the present study provide valuable insights into the potential benefits and risks associated with the cryogenic cooling of Li-ion batteries, contributing to the ongoing efforts to ensure their safe and sustainable use.

2. Experimental methods

2.1. Sample selection and test procedure

The experimental sample range comprises three types of Li-ion cells, differing in format, electrode chemistry, and capacity. Table 1 contains the relevant parameters of the cells related to this study.

For each cell type, a set of ten samples was divided into a test group ($n_T = 5$) and a reference group ($n_R = 5$). The reference samples were subjected to the same electrochemical test protocol without exposure to LN_2. An illustration of the study's test protocol can be found in Fig. 1.

2.2. Cryogenic experiments

The main cryogenic freezing tests of the samples were conducted by submerging them into a dewar vessel (Apollo 100, KGW-Isotherm Karlsruher Glastechnisches Werk – Schieder GmbH, Germany) filled with LN_2. A 3D-printed cell fixture, illustrated in Fig. 2, was used to submerge all test cells simultaneously. Additional cooling tests (outside the main test protocol) were performed in a dry-shipping cryogenic tank (Voyageur 5, Cryopal S.A., France) under gaseous nitrogen.

A freezing cycle consisted of three sequential submerging events of 30 min each, followed by a 90-min rethermalization period at room temperature. The waiting times were chosen to ensure sufficient freezing through the small samples [11] and were further confirmed by additional tests on a sample A cell equipped with an internal thermocouple. The thermocouple (type K) was inserted into the center of the cell through a small slit, which was tape-sealed afterward. The corresponding results are depicted in Figure S1 in the supporting information. Nonetheless, longer (re-)thermalization periods could be necessary for larger cell types. All cryogenic cooling tests were performed at an SOC of 50%, based on the discharge capacity determined during the previous characterization. Electrical and electrochemical characterization was conducted on all samples (test and reference group) before and after each cooling test cycle at $T = 20$ °C.

Table 2
EIS parameters for the tested cells.

Parameter	Cell type A	Cell type B	Cell type C
Frequency range	50 kHz–5 mHz	10 kHz–10 mHz	10 kHz–10 mHz
Excitation amplitude	2 mV	5 mV	5 mV
Points per decade	10	10	10

2.3. Electrochemical characterization

The electrochemical impedance spectroscopy (EIS) data were collected using a potentiostat (Interface 5000E, Gamry Instruments, USA) in a temperature chamber (LabEvent L T/150/70/3, Weiss Technik GmbH, Germany). The potentiostatic EIS (PEIS[1]) was conducted at a temperature of 20 °C and an SOC of 50%. The cell-specific EIS parameters can be extracted from Table 2.

Each electrical cycling test consisted of 10 cycles at a temperature of 20 °C. The first nine cycles were performed with a charge/discharge

[1] Compared to galvanostatic EIS (GEIS), which is often used for Li-ion cells with very low impedances, PEIS tends to be more robust for high-impedance systems, such as defect or cooled-down cells.

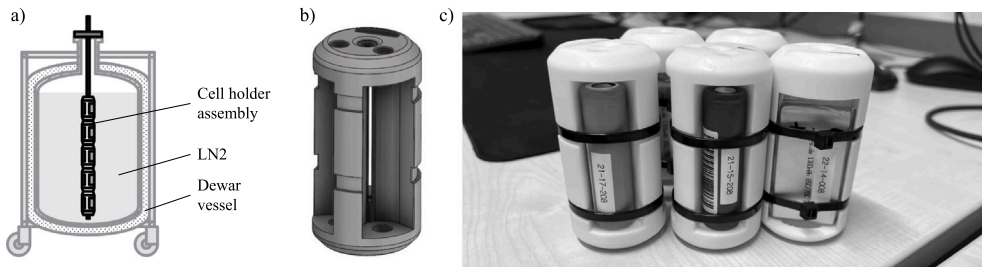

Fig. 2. Cooling test setup. For the cooling tests, the cells were submerged in an LN_2-filled dewar vessel (a). The cells were fixed by a 3D-printed cell holder (b and c).

rate of 1C, based on the battery's nominal capacity. In the last cycle, the rate was lowered to a C/10 rate. The charging step in each cycle was performed at a constant current (CC) until the cell-specific maximum voltage was reached. Subsequently, a constant-voltage (CV) step was performed until the current reached C/100 (CC-CV charge). For discharging the cell, a single CC step was applied (CC discharge).

For cell type A, a battery cycler (MCT-HD 20-6-2/96, Digatron Power Electronics, Germany) was used. The samples were kept at defined temperature conditions by employing a temperature chamber (LabEvent T/500/30/3, Weiss Technik GmbH, Germany) during cycling. Charge/discharge experiments of cell types B and C were performed by using a battery test system (BTS4000-5V12A, Neware Technology Limited, China) in combination with a temperature chamber (115l, F.lli Galli G. & P., Italy).

2.4. X-ray tomography

Extending the characterization of the cryogenic-frozen cells, X-ray computed tomography (XCT) was utilized to further evaluate the physical integrity of selected cells. For the XCT measurements, a µCT scanning system was utilized. The system consists of a microfocus X-ray tube (X-ray WorX GmbH, Germany) and a flat panel detector (PerkinElmer Inc., USA) with a resolution of 2048 × 2048 pixels. The tests were conducted at an operation voltage of 190 kV. The data was reconstructed using an in-house developed analysis tool based on the FDK[2] algorithm [13].

2.5. Gas chromatography

Gas analysis of swollen type A cells was performed using gas chromatography (GC). A Nexis GC-2030 (Shimadzu Corp., Japan) system with a Rt-Q-BOND PLOT column and a dielectric barrier discharge ionization detector (BID) was used for the measurements. The tests were performed on injected samples (injection temperature of 80 °C) with a volume of 200 µl and retention times up to 26 min.

3. Results and discussions

The capacity was monitored during cycling to quantify the electrochemical and electrical durability of Li-ion cells exposed to LN_2, as shown in Fig. 3. To ensure comprehensiveness, the absolute capacity of the individual cells is included in the supporting information in Figure S2.

During the experimental protocol, the relative capacity of the test samples of type A (pouch cell) decreased notably with an increasing variance among the samples compared to the reference group. The remaining capacity reached (98.1 ± 0.9) % for the test group and (99.6 ± 0.1) % for the reference group.

For cell type B (cylindrical cell), both groups show a peculiar capacity fade during the cycling tests whereas the test samples appeared to perform slightly worse than the reference cells. However, three test group samples failed[3] during the cycling tests (after the second cooling test cycle) so the quantitative comparison ($n_T = 2$ vs. $n_R = 5$) should be taken with caution.

Table 3
Remaining, relative discharge capacity after conducting the test protocol ($n = 5$).

Group	Cell type A	Cell type B	Cell type C
Reference group	(99.6 ± 0.1)%	(94.1 ± 2.4)%	(103.3 ± 0.2)%
Test group	(98.1 ± 0.9)%	(91.2 ± 0.9)%[a]	(103.4 ± 0.5)%[b]

[a] $n = 2$.
[b] $n = 4$.

Remarkably, the capacity of all type C samples — also cylindrical cells — increased gradually during the cycling. While this effect was not investigated further it is assumed that the increasing trend could have been caused by porosity changes and/or electrode wetting during the cycle tests, leading to an improved ionic conductivity. Similar to cell type B, one of the test samples failed after the second cooling test.

In summary, the relative capacity of cell type A decreased as a result of exposure to LN_2. The changes in the capacities of cell types B and C cannot be assigned unambiguously to the cooling tests and are listed in Table 3.

Contrarily to the observed capacity behavior during the cycling tests, the EIS data of cell type A in Fig. 4a appeared to be almost entirely unaffected by the cryogenic cooling tests.

Cell type B showed minor impedance changes in frequency ranges attributed to charge transfer, indicating a slightly decreased charge-transfer resistance. However, the non-functional cells were not part of the impedance comparison illustrated in Fig. 4b, decreasing the sample size significantly.

The slight impedance deviations for cell type C appear to be an offset of around 1.7 mΩ in the real part, which can be explained by a decrease in conductivity. Such artifacts can be caused by contact resistances inside the cells which behave like ohmic resistors (e.g., current collectors, tabs, etc.) and thus are not directly part of the electrochemical reactions.

The apparently unaffected impedance of cell type A — while experiencing significant capacity fade at the same time — seems contradictory. Despite the fact that electrode degradation (e.g., particle cracking with subsequent passivation layer growth) and changes in the electrolyte are discussed in the literature [6], the exact source of the mismatch between capacity and impedance remains unclear.

To investigate the aforementioned failure of four samples (three type B cells and one type C cell, all cylindrical) in detail, the integrity of the Li-ion cells was further assessed by observing their physical appearance after each freezing test cycle. While the non-functional cylindrical cells (type B and C) showed a bulging at the negative terminal, no physical changes were observed for cell type A (pouch cell)

[2] Developed at the Ford Motor Company, USA by L. A. Feldkamp, L. C. Davis, and J. W. Kress (FDK) [12].

[3] The failed/non-functional cells showed an open-circuit voltage of about 1 V but were otherwise not accepting any significant charge or discharge.

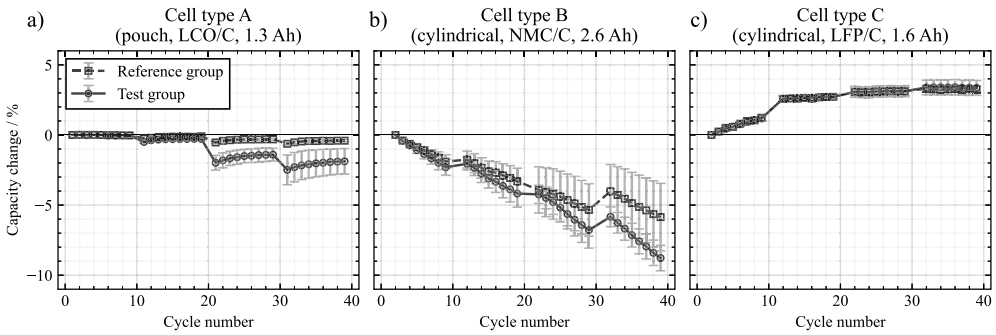

Fig. 3. Capacity data during the cycling tests. Trend of mean relative discharge capacities (1C) during cycling tests of (a) LCO/C pouch cells, (b) NMC/C cylindrical cells, and (c) LFP/C cylindrical cells. After the second freezing test cycle (cycle number 20 of the cycling test) three type B cells and one type C cell failed and were excluded from the subsequent testing.

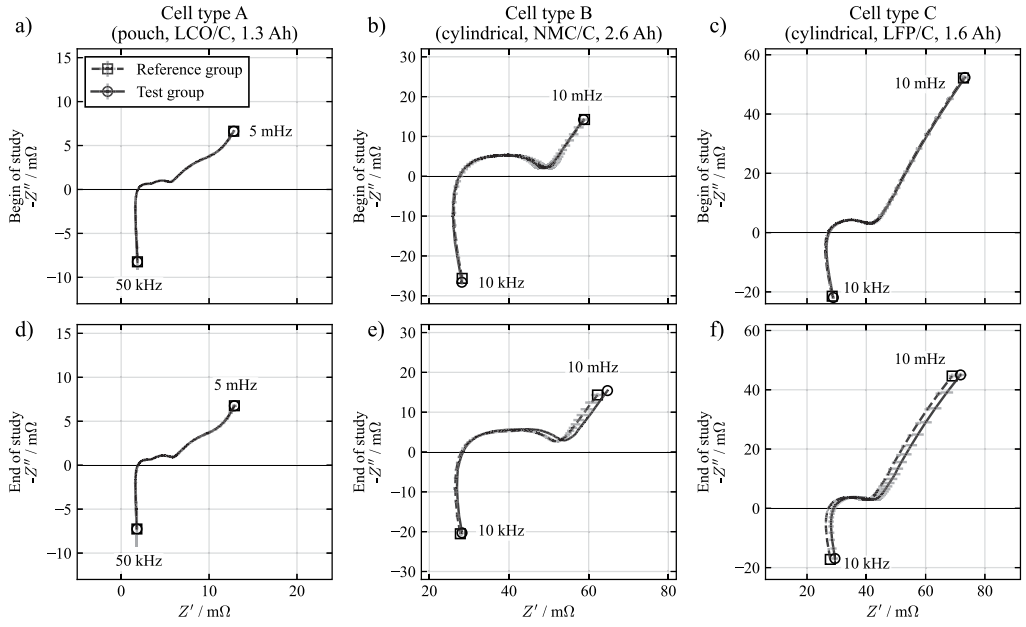

Fig. 4. Impedance data of tested cells. Nyquist plots received from EIS measurements at begin (a, b, and c) and at the end of the study (d, e, and f) for cell types A (a and d), B (b and e), and C (c and f). Cell type A shows no significant differences between test and reference group. Cell type B shows slight differences in the charge-transfer behavior. The impedance of cell type C indicates a real-part offset of 1.7 mΩ compared to the reference samples.

during the scheduled cooling tests. However, additional experiments on type A cells with a deliberately longer exposure (>18 h) to LN_2 led to an intense swelling after rethermalization to ambient temperature, as depicted in Fig. 5.

Apparently, the major swelling of the type A cell is accompanied by a change of impedance. Alternating current (AC) and direct current (DC) characterization were utilized to determine the alterations. The corresponding data, which is depicted in Figure S3 in the supporting information, indicates that the observed changes are mainly due to a shift of Ohmic resistance. Interestingly, similar alterations were not observed for the samples exposed to LN_2 for only 30 min — even after several cryogenic cooling cycles.

If the swelling could be attributed to degradation effects occurring during rethermalization after cryogenic freezing, the internal gas formation should be more severe with repeated freezing-thawing-cycles. Moreover, the duration of freezing should not affect gas formation upon reaching constant cryogenic temperatures. However, the results of cell type A clearly show that even multiple freezing-thawing-cycles did not lead to any visible swelling, whereas storing the cell once in LN_2 for a longer period resulted in a large expansion of the cell. Considering the severely reduced (electro)chemical reaction kinetics inside a cell at cryogenic temperatures, only leaked-in N_2 remains as a possible explanation for the observed effects.

Furthermore, a similar swelling behavior — though to a less severe extent — was also reproduced by exposing samples to a gaseous nitrogen atmosphere (below −190 °C) in a dry-shipping container for 12 h, confirming that expansion is not exclusive to exposure to nitrogen in its liquid phase.

Leaked-in N_2 as the main cause of swelling in cell type A also hints towards a similar origin for the observed swelling in the failed type B and C (cylindrical) samples. For these samples, the overpressure was likely caused by differently shrunken components at the positive electrode[4] during freezing.

To gain further insights, the gas extracted from a swollen type A cell exposed to N_2 for >18 h was analyzed using GC. For comparison, a second measurement was performed on the gas extracted from a different, deliberately degraded, sample of the same type. The corresponding results are depicted in Figure S4 in the supporting information. The LN_2 sample exhibited twice the detected, relative N_2 signal compared to its degraded counterpart, which, on the other hand, showed larger signals attributed to gases such as CH_4, CO_2, and — as a typical product

[4] Typical materials used at the positive electrode of cylindrical cells are aluminum ($\alpha = 32 * 10^{-6}\,K^{-1}$) or stainless steel ($\alpha = 13 * 10^{-6}\,K^{-1}$) for the housing, and polypropylene ($\alpha > 100 * 10^{-6}\,K^{-1}$) for the gasket.

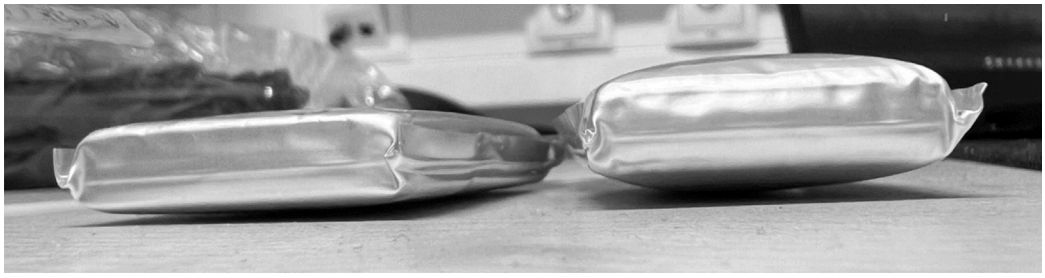

Fig. 5. Side view of cell type A. Reference cell (left) and swollen cell after exposure to LN_2 for >12 h (right).

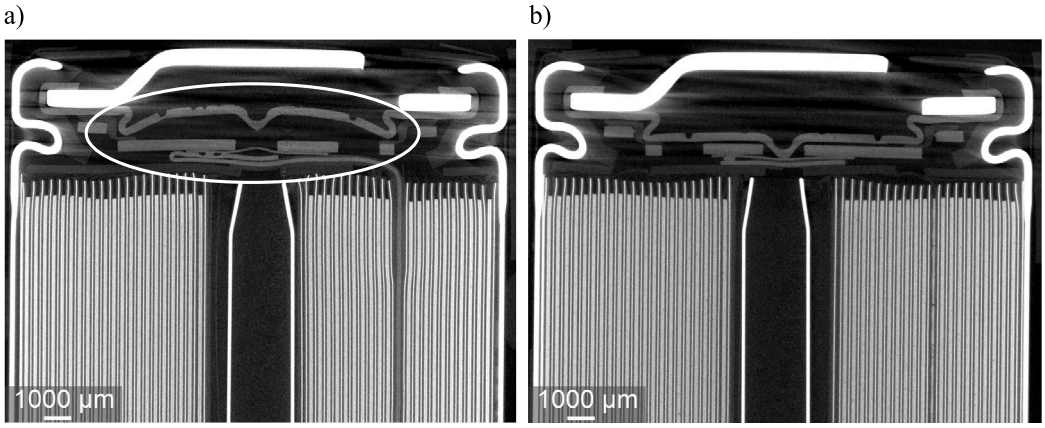

Fig. 6. X-ray computed tomography (XCT) images of tested samples. XCT of a non-functional type B cell (a) compared to a reference cell (b). The first cell shows an activated current interrupt device (CID, highlighted) which is triggered by overpressure inside the cell. In the particular cell, the overpressure is assumed to be caused by nitrogen leaking into the cell during the cooling tests which subsequently expands (during the rethermalization). Material changes cannot be observed.

of electrolyte-related degradation — H_2. This further supports that leaked-in N_2 caused the swelling of the cell.

The observed impedance changes in the sample exposed to LN_2 could be the result of a decrease in layer connectivity due to inserted N_2. Furthermore, it has to be considered, that N_2 can also react with the lithiated graphite in the negative electrode, resulting in cell degradation [14].

To further assess if the swelling observed for pouch cell type A is also responsible for the failure of the cylindrical cell types B and C, two cells were investigated using XCT.

The non-functional cell in Fig. 6 shows an activated current interrupt device (CID). Otherwise, no implications of structural changes were seen. The CID is a safety mechanism that disconnects the positive electrode's current collector from the positive terminal when pressure builds up inside the cell.

To finally determine whether the observed swelling is caused by internal decomposition effects or by leaked-in nitrogen, the non-functional cells were manually revived by resetting their CID. Reviving the cells was done by puncturing the cell terminal to release the internal overpressure and pushing back — hence deactivating — the CID. The resulting hole was temporarily sealed using polyimide film tape. Since subsequent voltage readings on the reactivated samples resembled those of normal working cells, the previously observed non-functional behavior of the samples was assumed to be related to the activated CID.

To support the assumption, EIS measurements were performed for cells with an active CID (still non-functional sample) and a deactivated CID (reactivated sample). Furthermore, an extracted positive terminal (with the CID still attached) was tested to exclude possible electrochemical effects. Anticipating extraordinarily high — yet purely ohmic — impedances for the non-functional samples and the isolated terminal, regular impedances were expected for the punctuated (thus reactivated) cells. Respective results are depicted in Fig. 7.

Fig. 7a shows an exceptionally high — peculiarly not purely ohmic — impedance (MΩ range) for a non-functional cell with an active CID. Contradicting the aforementioned anticipation, features of a charge transfer reaction were found. Since this quantity was also strongly temperature dependent, a remaining electrochemical activity was initially presumed. However, additional experiments — decoupling the active material and the CID by physically separating them — showed a similar behavior when the tab was flooded with electrolyte. Nonetheless, no sign of a charge transfer reaction was found when kept in a dry state, as shown in Fig. 7b. Finally, manually resetting the CID led to the vanishing of any unusual impedance characteristics, and the EIS response of a fully functional cell was obtained as depicted in Fig. 7c. Moreover, the impedance behavior of the reactivated cell nicely overlaps with the data of a reference cell, thus, clearly supporting the initial assumption (based on the voltage readings) that the LN_2-induced effects can be reversed by a simple pressure release.

These findings led to the final conclusion that an activated CID, filled with electrolyte, acts as an additional electrochemical interface which may be misinterpreted as a remaining electrochemical activity. Furthermore, they demonstrate that the observed swelling cannot be assigned to any electrochemical changes inside the cells and thus support the idea of nitrogen intrusion at cryogenic temperatures. Other possible sources of internal overpressure (such as internal gas evolution due to electrolyte decomposition) would likely induce severe lasting changes in the electrochemical behavior and are, however, not observed.

4. Conclusions

In the present study, three different types of Li-ion cells (type A, pouch, LCO/C; type B, cylindrical, NMC/C, and type C, cylindrical,

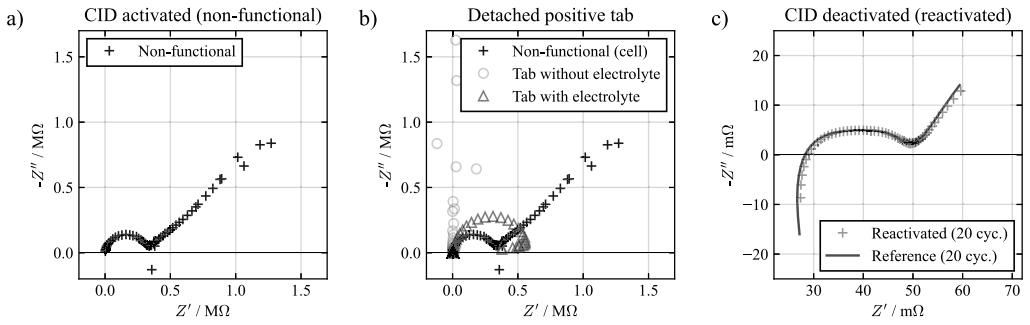

Fig. 7. Impedance data of non-functional cells. Nyquist plot of a non-functional type B cell (a). Subsequently, the positive terminal assembly was detached from a non-functional cell and tested separately with and without added electrolyte (b) to eliminate electrochemical effects. A noticeable capacitive behavior can be observed for the positive tab in the presence of electrolyte. Additionally, a reactivated cell is compared to a reference cell (c). The measurement parameters can be extracted from Table 2.

LFP/C) were subjected to rapid freezing tests to assess their electrochemical and physical stability at cryogenic temperatures potentially suited for transportation and storage. For each type, the cells were divided into a test group and a reference group. The latter was subjected to the same electrochemical test protocol without cryogenic tests. The impedance of cells of type A showed no significant changes upon exposure to liquid nitrogen (LN_2), however, their final capacity deviates noticeably when compared to their reference analogs. While the capacity changes of cell types B and C cannot be directly attributed to the exposure to LN_2, their impedance data show minute changes in the charge transfer resistance and ohmic resistance, respectively.

Interestingly, four of the tested cylindrical cells failed in the course of this study. While the pouch cells under investigation retained their functionality during the tests, exposing them to LN_2 for extended periods led to significant swelling after rethermalization. Due to the possibility to reactivate the non-functioning cells to a functional, non-altered state, according to EIS measurements, the observed effect can be linked to nitrogen leaking into the cells during the cryogenic freezing steps. This implies that all three tested cell types are prone to nitrogen intrusion when cooled down rapidly.

In this manner, it is shown that direct cooling on a cell level with LN_2 is not suited for enhancing the safety of the transport and/or storage of lithium-ion batteries without limitations if subsequent electrochemical use of the cells is intended. Despite the fact that the electrochemical characteristics remain largely unaffected, the physical integrity of the cell housing suffers from cryogenic freezing which can trigger internal safety mechanisms. This can ultimately create a false impression of safety as Li-ion cells — still holding their energy internally — might appear non-functional or, more precisely, in a deep-discharge state.

CRediT authorship contribution statement

R. Leonhardt: Formal analysis, Software, Visualization, Writing – original draft. **N. Böttcher:** Investigation, Validation, Writing – original draft. **S. Dayani:** Resources, Writing – review & editing. **A. Rieck:** Resources, Writing – review & editing. **H. Markötter:** Resources, Writing – review & editing. **A. Schmidt:** Funding acquisition, Project administration. **J. Kowal:** Methodology, Supervision, Writing – review & editing. **Tim Tichter:** Supervision, Writing – original draft. **Jonas Krug von Nidda:** Conceptualization, Project administration, Writing – original draft.

Declaration of competing interest

The authors declare that they have no known competing financial interests or personal relationships that could have appeared to influence the work reported in this paper.

Data availability

Data will be made available on request.

Acknowledgments

The authors acknowledge the Austrian Federal Ministry of Climate Action, Environment, Energy, Mobility, Innovation and Technology for supporting the project “SafeLiBatt” (FFG project no. 880683), the Bundesanstalt für Materialforschung und -prüfung (BAM), and the French National Institute for Industrial Environment and Risks (INERIS), who finance the transnational funding program SAF€RA.

Appendix A. Supplementary data

Supplementary material related to this article can be found online at https://doi.org/10.1016/j.est.2024.111650.

References

[1] M. Slattery, J. Dunn, A. Kendall, Transportation of electric vehicle lithium-ion batteries at end-of-life: A literature review, Resour. Conserv. Recy. 174 (2021) 105755, http://dx.doi.org/10.1016/j.resconrec.2021.105755.
[2] A. Nedjalkov, J. Meyer, M. Köhring, A. Doering, M. Angelmahr, S. Dahle, A. Sander, A. Fischer, W. Schade, Toxic gas emissions from damaged lithium ion batteries—Analysis and safety enhancement solution, Batteries 2 (2016) 1–10, http://dx.doi.org/10.3390/batteries2010005.
[3] D. Wei, M. Zhang, L. Zhu, H. Chen, W. Huang, J. Yao, Z. Yuan, C. Xu, X. Feng, Study on thermal runaway behavior of li-ion batteries using different abuse methods, Batteries 11 (2022) 201, http://dx.doi.org/10.3390/batteries8110201.
[4] Y. Cao, K. Wang, Z. Wang, J. Wang, Y. Yang, X. Xu, Utilization of liquid nitrogen as efficient inhibitor upon thermal runaway of 18650 lithium ion battery in open space, Renew. Energy 206 (2023) 1097–1105, http://dx.doi.org/10.1016/j.renene.2023.02.117.
[5] Z. Wang, K. Wang, J. Wang, Y. Yang, Y. Zhu, W. Bai, Inhibition effect of liquid nitrogen on thermal runaway propagation of lithium ion batteries in confined space, J. Loss Prev. Process Ind. 79 (2022) 104853, http://dx.doi.org/10.1016/j.jlp.2022.104853.
[6] J. Li, S. Li, Y. Zhang, Y. Yang, S. Russi, G. Qian, L. Mu, S.-J. Lee, Z. Yang, J.-S. Lee, P. Pianetta, J. Qiu, D. Ratner, P. Cloetens, K. Zhao, F. Lin, Y. Liu, Multiphase, multiscale chemomechanics at extreme low temperatures: Battery electrodes for operation in a wide temperature range, Adv. Energy Mater. 11 (2021) 2102122, http://dx.doi.org/10.1002/aenm.202102122.
[7] T.R. Grandjean, J. Groenewald, A. McGordon, J. Marco, Cycle life of lithium ion batteries after flash cryogenic freezing, J. Energy Storage 24 (2019) 100804, http://dx.doi.org/10.1016/j.est.2019.100804.
[8] T.R. Grandjean, J. Groenewald, J. Marco, The experimental evaluation of lithium ion batteries after flash cryogenic freezing, J. Energy Storage 21 (2019) 202–215, http://dx.doi.org/10.1016/j.est.2018.11.027.
[9] N. Sunderlin, A. Colclasure, C. Yang, J. Major, K. Fink, A. Saxon, M. Keyser, Effects of cryogenic freezing upon lithium-ion battery safety and component integrity, J. Energy Storage 63 (2023) 107046, http://dx.doi.org/10.1016/j.est.2023.107046.
[10] K. Nandini, K. Usha, M. Srinivasan, M. Pramod, P. Satyanarayana, M. Sankaran, Study on survivability of 18650 lithium-ion cells at cryogenic temperatures, J. Energy Storage 17 (2018) 409–416, http://dx.doi.org/10.1016/j.est.2018.03.018.

[11] J. Kowal, A. Arzberger, H. Blanke, D.U. Sauer, How to determine the time for temperature equalisation in batteries and supercaps for reliable laboratory measurements, J. Energy Storage 4 (2015) 113–120, http://dx.doi.org/10.1016/j.est.2015.09.009.

[12] L.A. Feldkamp, L.C. Davis, J.W. Kress, Practical cone-beam algorithm, J. Opt. Soc. Amer. 1 (1984) 612–619, http://dx.doi.org/10.1364/JOSAA.1.000612.

[13] S. Dayani, H. Markötter, A. Schmidt, M.P. Widjaja, G. Bruno, Multi-level X-ray computed tomography (XCT) investigations of commercial lithium-ion batteries from cell to particle level, J. Energy Storage 66 (2023) 107453, http://dx.doi.org/10.1016/j.est.2023.107453.

[14] H. Wang, W.-D. Zhang, Z.-Q. Deng, M.-C. Chen, Interaction of nitrogen with lithium in lithium ion batteries, Solid State Ion. 180 (2009) 212–215, http://dx.doi.org/10.1016/j.ssi.2008.12.001.